

# Methanol and ethanol conversion into hydrocarbons over H-ZSM-5 catalyst

S. Hamieh<sup>1</sup>, C. Canaff<sup>1</sup>, K. Ben Tayeb<sup>2</sup>, M. Tarighi<sup>1</sup>, S. Maury<sup>3</sup>, H. Vezin<sup>2</sup>,  
Y. Pouilloux<sup>1</sup>, and L. Pinard<sup>1,a</sup>

<sup>1</sup> IC2MP, UMR 7285 CNRS – Université de Poitiers, 4 rue Michel Brunet, 86073 Poitiers, TSA 51106, France

<sup>2</sup> LASIR, UMR 8516 CNRS – Université de Lille 1, Bâtiment C4, 59655 Villeneuve d'Ascq Cedex, France

<sup>3</sup> IFP Energies Nouvelles, Rond-point de l'échangeur de Solaize, BP. 3, 69360 Solaize, France

Received 23 November 2014 / Received in final form 21 May 2015  
Published online 30 July 2015

**Abstract.** Ethanol and methanol are converted using H-ZSM-5 zeolite at 623 K and 3.0 MPa into identical hydrocarbons (paraffins, olefins and aromatics) and moreover with identical selectivities. The distribution of olefins as paraffins follows the Flory distribution with a growth probability of 0.53. Regardless of the alcohol, the catalyst lifetime and selectivity into hydrocarbons C<sub>3+</sub> are high in spite of an important coke content. The coke that poisons the Brønsted acid sites without blocking their access is composed in part of radical polyalkylaromatics. The addition of hydroquinone, an inhibitor of radicals, to the feed, provokes an immediate catalyst deactivation.

## 1 Introduction

Both ethanol, a fermentation product of biomass [1,2], and methanol, synthesized from syngas [3,4], can be further converted into olefins and hydrocarbons using zeolites as acid catalysts [5–10]. In 2009, Christensen and coll. have shown that the conversion of Ethanol-To-Gasoline over an H-ZSM-5 catalyst yielded essentially to the same product distribution as for Methanol-To-Gasoline [11]; they concluded that both methanol (MeOH) and ethanol (EtOH) go through similar reaction mechanism to form hydrocarbons in gasoline range. Consequently, the reaction, conducted on a mixture of MeOH and EtOH, is likely one of the best way to incorporate a large portion of renewable carbon into synthetic fuels. It is surprising to obtain such results since the two reactants do not have the same nature; EtOH which undergoes easy dehydration at moderate temperature can be considered as an equimolar mixture of water and ethylene rather than as an alcohol [12].

To explain the similarity in the reaction products, it can simply assume that ethylene (C<sub>2</sub>H<sub>4</sub>) is the reaction intermediate of MeOH transformation into hydrocarbons.

<sup>a</sup> e-mail: ludovic.pinard@univ-poitiers.fr

**Table 1.** Physicochemical properties of the HZSM-5(40) zeolite.

Si/Al ratio <sup>a</sup>	Crystal size <sup>b</sup> (nm)	V <sub>micro</sub> <sup>c</sup> (cm <sup>3</sup> .g <sup>-1</sup> )	V <sub>meso</sub> <sup>d</sup> (cm <sup>3</sup> .g <sup>-1</sup> )	S <sub>ext</sub> <sup>c</sup> (m <sup>2</sup> .g <sup>-1</sup> )	[PyH <sup>+</sup> ] <sup>e</sup> (μmol.g <sup>-1</sup> )	[PyL] <sup>e</sup> (μmol.g <sup>-1</sup> )
40	580	0.177	0.085	85	297	47

<sup>a</sup> Elemental analysis, <sup>b</sup>SEM, <sup>c</sup>Micropore volume and external surface calculated using the t-plot method;

<sup>d</sup> Mesopore volume = V<sub>total</sub> - V<sub>mic</sub> (V<sub>total</sub>: the volume adsorbed at P/P<sub>0</sub> = 0.99); <sup>e</sup> Concentrations of Brønsted (Py H<sup>+</sup>) and Lewis (Py L) sites able to retain pyridine at 423 K.

CH<sub>3</sub>OH follows an intermolecular dehydration pathway to form dimethyl ether before forming C<sub>2</sub>H<sub>4</sub>, then it goes on through oligomerization, dehydrocyclization and hydrogenation reactions to form a complex mixture of gasoline-range hydrocarbons [13]. Dehydration reactions take place on weak acidic sites, whereas others reactions require sites with stronger acid strength [13,14].

But, it is generally accepted in the open literature that the olefins in MeOH conversion arise from a “pool”, i.e. a large range of polyalkylaromatic species in the catalyst [15,16]. According to Kolboe and co-workers [8,17,18], the formation of the C-C bond begins by an acid alkylation of a methoxy group on an aromatic compound. The location of polymethylbenzenes in the small channel intersections of H-ZSM-5 zeolite, limits their condensation but promotes their isomerization. This medium pore size zeolite, owing to its specific topology, leads through a paring mechanism of the aromatic ring to the growth of side chains (propyl, butyl, tertbutyl and isopentyl) that are released as olefins by β-scission. The mechanism of alcohols transformation involves that the acidic hydroxyl groups react with alcohols to alkylate or rather feed continuously the aromatic rings with methyl groups. The chemical nature of hydrocarbon pool (cationic, neutral, radical) is still under debate. Kim et al. have evidenced, by Electron Paramagnetic Resonance (EPR) spectroscopy, the generation of hexamethylbenzenium (HMB<sup>+•</sup>) radical cation during MTO reaction [19]. Ben Tayeb et al. showed by *in situ* EPR spectroscopy that a fraction of radicals was consumed during ethene oligomerisation at 723 K [6]. In previous work, the participation of radicals in ETH (ethanol-to-hydrocarbons) “pool mechanism” was highlighted by adding hydroquinone (a radical inhibitor, HQ) to the feed gas; the consumption of radical species by HQ enhanced the catalyst deactivation [20].

The aim of this study is to understand the impact of HQ in the methanol transformation both on stability, activity and selectivity of the catalyst, and on composition, location and nature of coke. The experimental data will be compared with those previously obtained and published, on the role of radicals in ethanol transformation [20].

## 2 Experimental part

### 2.1 Catalytic tests

The starting ZSM-5 sample (Si/Al = 40, crystallite size = 580 nm) was supplied by Zeolyst (CBV8020) in his ammonium form. Prior to use, the catalyst was compacted, crushed and sieved in order to get 0.2–0.4 mm particles. The protonic zeolite form (HZSM-5) was obtained, before catalytic testing, by *in situ* activation under nitrogen (3.3 L h<sup>-1</sup>, 30 bar) at 773 K during 12 h; its physicochemical properties (crystallite size, pore volume and acidity) are reported in Table 1.

The catalytic tests were carried out in a continuous down-flow fixed bed reactor. The operating conditions for alcohol transformations were as follows: 623 K, 30 bar total pressure, N<sub>2</sub>/alcohol (MeOH or EtOH) molar ratio = 4, gas hourly space velocity

(GHSV) =  $5.3 \text{ h}^{-1}$ . In the radical poisoning tests 1 and 2 wt.% of hydroquinone (Acros Organics, 99.5% pure) were dissolved in alcohol. Spent catalysts were recovered at the end of each experiment following reactor cool-down to room temperature. The reaction products were analysed on-line using a VARIAN 3800 gas chromatograph equipped with two detectors: a FID connected to a J&W PONA capillary column, and a TCD connected to a double column composed of a 5A sieve and a Porabond Q.

## 2.2 Spent catalyst characterization

The carbon content was measured using a full burning at 1293 K with a mixture of helium and oxygen in a Thermoquest NA2100 analyzer.

Prior to measuring their residual acidity and porosity, the spent catalysts were outgassed first at 363 K for 1 h, then at 423 K for another hour, whereas the fresh catalyst were outgassed at 523 K overnight. Infrared spectra (FTIR) of adsorbed pyridine (373 K) were recorded on a Nicolet Magna 550-FT-IR spectrometer with a  $2 \text{ cm}^{-1}$  optical resolution. After establishing a pressure of 1 Torr at equilibrium, the cell was evacuated at 423 K to remove all physisorbed species. The amount of pyridine adsorbed on the Brønsted and Lewis sites was determined by integrating the band areas at respectively  $1545 \text{ cm}^{-1}$  and  $1454 \text{ cm}^{-1}$  and using the following extinction coefficients:  $\varepsilon_{1545} = 1.13$  and  $\varepsilon_{1454} = 1.28 \text{ cm} \cdot \text{mol}^{-1}$ . A Micromeritics 2020 ASAP was used for nitrogen sorption measurements. Specific surface areas were determined from the BET equation. The total volume corresponds to nitrogen adsorbed at  $P/P_0 = 0.99$  and the  $t$ -plot method was used to distinguish micropores from mesopores.

The concentration of radicals was measured at room temperature directly on the spent catalyst by EPR spectroscopy using a Bruker ELEXSYS E500 spectrometer operating in X-band. The spectra were recorded at a 100 KHz modulation field frequency with an amplitude modulation of 0.1 mT and a microwave power of 5 mW corresponding to non-saturation conditions. The Weak Pitch from Bruker was used as standard reference and contained a known concentration of spin/mass ( $1.29 \cdot 10^{13} \text{ spins g}^{-1}$ ). It was analysed under the same operating conditions as the catalysts. The spin concentration is given by the double integration of the first derivative of the EPR signal.

The chemical composition of coke was determined using the method developed in Poitiers [21,22]. The zeolite was dissolved at room temperature with a 51 wt.% hydrofluoric acid (HF) solution to release, without modification, the molecules trapped in the pores. Then, the coke molecules soluble in methylene chloride were analyzed by GC-MS ("Thermo Electron DSQ" equipped with a DB5ms column). For MALDI-TOF MS, 10 mg of the extract was suspended in  $500 \mu\text{L}$  of THF and was mixed with Dithranol as MALDI matrix ( $5 \text{ g} \cdot \text{L}^{-1}$  in THF). After sonication, about  $0.5 \mu\text{L}$  of this mixture was hand spotted onto the stainless steel target and dried at room temperature. MS was performed on a Bruker Autoflex Speed mass spectrometer in a reflectron positive mode where ions were generated by a 337 nm wavelength nitrogen laser. Analyses were achieved using pulsed ion extraction (delay time 130 ns). The laser power was adjusted slightly above the threshold of the desorption/ionization process and the spectra were the sum of 40 000 shots.

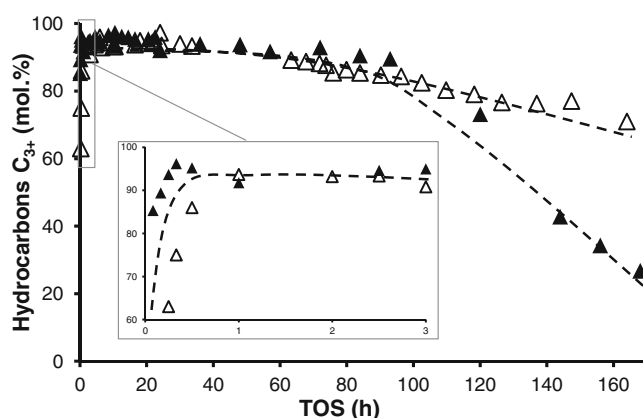
## 3 Results

### 3.1 Catalyst lifetime and products distribution

MeOH and EtOH transformations were carried out at 623 K under 3.0 MPa of total pressure. Alcohol conversions were always complete. The reaction products were  $\text{H}_2\text{O}$ ,

**Table 2.** EtOH and MeOH conversions, and yields (mol.%) into methane ( $\text{CH}_4$ ), ethylene ( $\text{C}_2\text{H}_4$ ), ethane ( $\text{C}_2\text{H}_6$ ), dimethylether (DME) and diethylether (DEE), obtained after 2, 24, 72 and 168 h on stream. ETH data from [20].

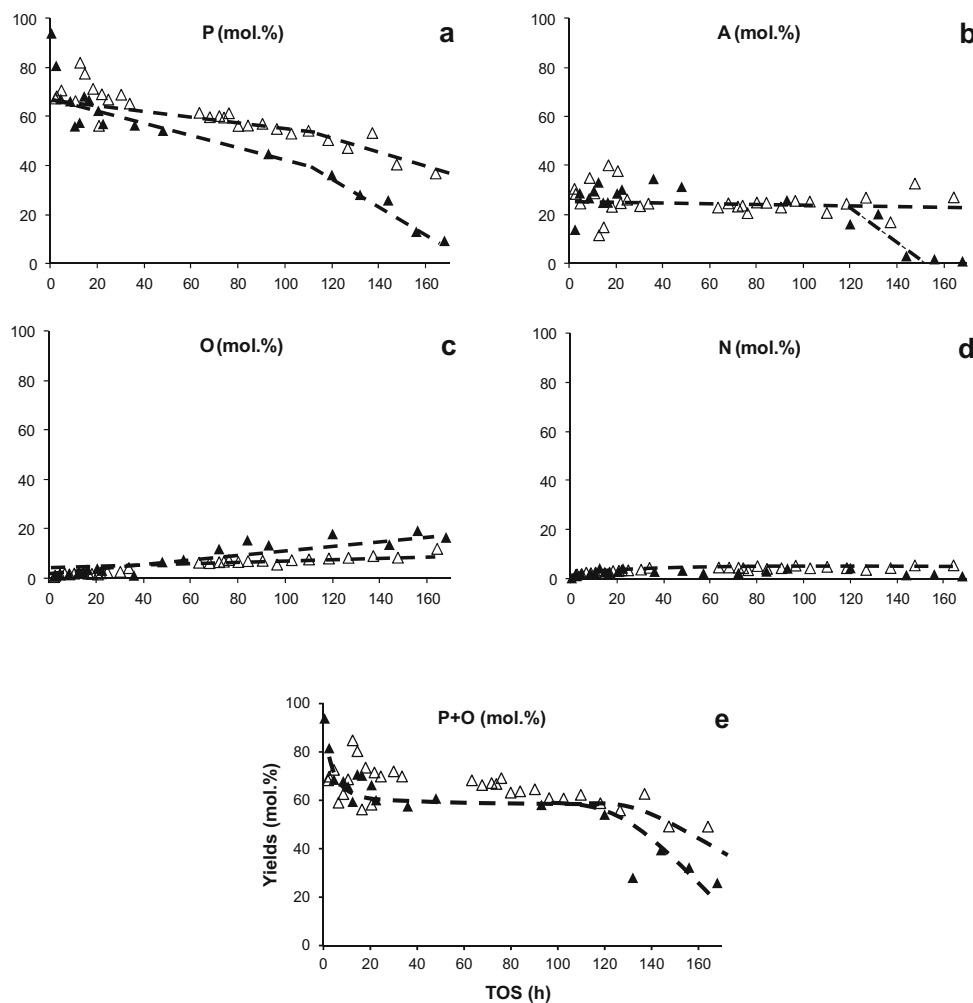
Reactant	MeOH				EtOH			
	2	24	72	168	2	24	72	168
TOS (h)	2	24	72	168	2	24	72	168
Conv. (%)	100	100	100	100	100	100	100	100
DME/DEE	0	0.1	0.0	4.3	0.3	0	0	0.0
$\text{CH}_4$	3.9	3.8	3.6	3.2	1.3	1.2	0.5	1.4
$\text{C}_2\text{H}_4$	1.0	1.6	7.4	21.7	0.6	0.9	2.6	73.4
$\text{C}_2\text{H}_6$	1.6	1.2	0.7	0	3.2	1.8	4.1	0.4
$\text{C}_{3+}$	93.2	93.5	88.2	71	94.2	94	92.9	26.8



**Fig. 1.** Yields (wt.%) into hydrocarbons  $\text{C}_{3+}$  as a function of time-on-stream (h). Tests performed at 623 K on H-ZSM-5 with MeOH ( $\Delta$ ) and EtOH ( $\blacktriangle$ ). ETH data from [20].

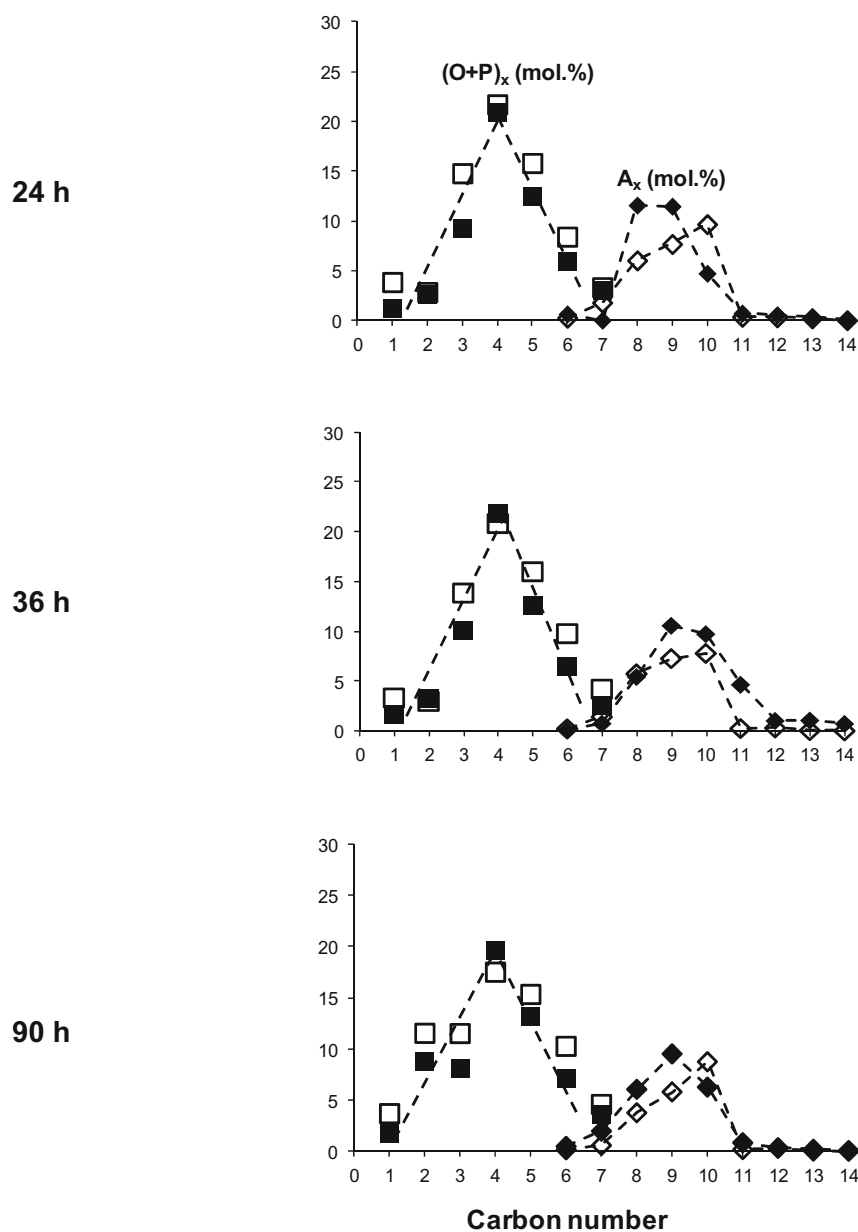
$\text{CH}_4$ ,  $\text{C}_2\text{H}_6$ ,  $\text{C}_2\text{H}_4$  and hydrocarbons with a carbon number higher than 2,  $\text{C}_{3+}$ ; (Table 2). The dehydration reactions involve weak acidic sites, whereas the transformation into longer hydrocarbons ( $\text{C}_{3+}$ ) occurs on strong acidic sites [13,14]. So, the catalyst stability is not related to the alcohol conversion but to the formation of  $\text{C}_{3+}$ . Figure 1 compares as a function of time-on-stream (TOS) the molar yields into  $\text{C}_{3+}$  obtained from MeOH and EtOH. After a fast induction period ( $\sim 1$  h), a long stationary state (or rather a very slow deactivating period) occurred during  $\sim 100$  h; the yields into  $\text{C}_{3+}$  were identical and around 94% with any alcohol. The  $\text{C}_{3+}$  yields are not total regardless of the TOS (initially or during the “pseudo” stationary state). This confirms that the catalytic behavior is not due to an oversizing of the MFI catalyst bed. The apparent stability was followed by a catalyst deactivation which was more accentuated with EtOH than MeOH. During the period of deactivation, the primary dehydration products appeared *i.e.* ethylene and diethylether (DEE) or dimethylether (DME) with methanol (Table 2). The  $\text{C}_{3+}$  products were classified by chemical family: paraffins (P), olefins (O), naphthenes (N) and aromatics (A).

Figure 2 reports the molar yields for each family as a function of time-on-stream. The yields of aromatics and naphthenes remained stable with TOS (25% and 4% respectively), whereas the yields of paraffins and olefins evolved. During the “pseudo” stationary state, the decrease of P (Fig. 2a), which was more important



**Fig. 2.** Yields (mol.%) into (a) Paraffins (P), (b) Aromatics (A), (c) Olefins (O), (d) Naphthenes (N), and (e) P + O as a function of time-on-stream (h). Tests performed at 623 K on H-ZSM-5 with MeOH ( $\triangle$ ) and EtOH ( $\blacktriangle$ ).

with EtOH than MeOH, coincided quantitatively with the increase of the yield into olefins (Fig. 2c); indeed the sum of O and P (Fig. 2e, S.I. 1 and S.I. 2) remained constant. The products evolution with time-on-stream shows that the formations of P and A are due to a fast hydrogen transfer between naphthenes and olefins. In Fig. 3, the molar yields of  $(P + O)_n$  and  $A_n$  are reported according to their carbon number ( $n$ ). Regardless both alcohols and time-on-stream, identical hydrocarbons were produced with the same selectivity. The distribution of  $(P + O)_n$  and  $A_n$  were centered to 4 and 9-10 carbon atoms respectively. The iso to normal ( $i/n$ ) ratios for 4 and 5 carbon atoms paraffins ( $P_4$  and  $P_5$ ) were higher than 2 with both alcohols (Fig. S.I.3); with EtOH,  $i/n$  was constant with TOS whereas with MeOH it continuously increased. It should be underscored that the product distribution of  $(P + O)_n$  follows the Flory distribution with a growth probability factor  $\alpha$  equal to 0.53 (Fig. 4). The mathematical Flory law describes the relative probability of chain growth versus chain termination and therefore, implies that products which are formed do not react further.



**Fig. 3.** Products distribution: Olefins + Paraffins  $(O + P)_n$  ( $\square$ ,  $\blacksquare$ ) and Aromatics ( $A_x$ ) ( $\diamond$ ,  $\blacklozenge$ ) obtained at 24, 36 and 90 h as a function of carbon number. Tests performed at 623 K on H-ZSM-5 with MeOH ( $\square$ ,  $\diamond$ ) and EtOH ( $\blacksquare$ ,  $\blacklozenge$ ).

### 3.2 Spent catalyst characterizations

The coke content was identical independently of the alcohol used, after a fast increase it reached a plateau at 11 wt.% after 72 h (Fig. 5a). The impact of coke, both on the pore volume (accessible to nitrogen) and on the concentration of protonic sites (able to retain pyridine adsorbed at 423 K) are shown as a function of the coke content in Fig. 5b and 5c. The residual pore volume ( $V_{mic}/V_0$ ) and residual acidity ( $C_H + /C_0$ )

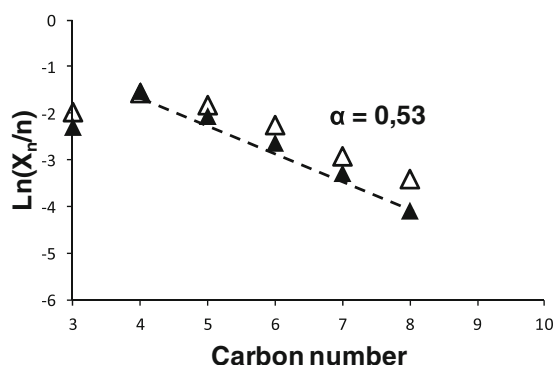


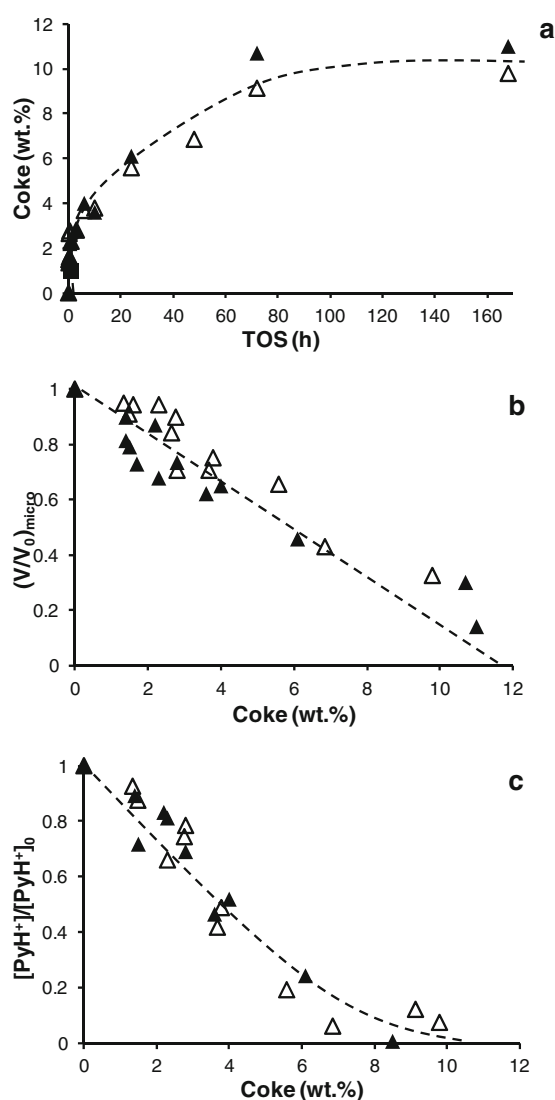
**Fig. 4.** Flory distribution of O+P as a function of carbon number,  $\alpha$  is the growth probability factor. Tests performed at 623 K on H-ZSM-5 with MeOH ( $\Delta$ ) and EtOH ( $\blacktriangle$ ).

were inversely proportional to the amount of carbon. The total poisoning of protonic sites and the total blockage of the access to the micropore were reached both at carbon content around 11 wt.%. No molecules can be recovered by washing of the spent zeolites; hence all coke molecules, even 150 h run are trapped in micropores. After dissolution of the coked zeolite by HF, the coke molecules were extracted by  $\text{CH}_2\text{Cl}_2$  and analyzed by GC-MS and MALDI-TOF MS (Table 3). The coke molecules formed during MTH (methanol-to-hydrocarbons) reaction were composed, after 24 h, mainly of tetra, penta and hexamethylbenzenes (Family A  $\sim$  60 mol.%) as well as polymethylated naphthalenes (Family B). This composition is usual for MTH reaction [12], while with EtOH the coke was slightly heavier. It was mainly constituted of bi rather tri aromatic rings (70–80 mol.%) substituted by many methyl and ethyl groups (Families B and C). Molecules with four rings (Family D) have also been detected. In spite of the differences in coke composition, the average molar mass of coke with the two reactants was estimated to  $200 \text{ g mol}^{-1}$ .

The coking of the zeolite led to the formation of free radicals [23, 24] which can be characterized and quantified by EPR spectroscopy. One part of polyaromatic molecules trapped in the zeolite pores could be spontaneous ionized into radical cations [25]. Moreover, the steric constraint limits the radical cations mobility, impeding the dimerization reaction. The radical cations trapped in the ZSM-5 pores are consequently stabilized [25]. The EPR spectral parameters measured at room temperature on spent catalysts with the same coke content ( $\sim$  6 wt.%) are summarized in Table 4. The spectra consisted in a single unresolved Lorentzian line centered at a  $g$  factor of 2.0026 and with a linewidth ( $\Delta H$ ) of 9.3–9.4 G. Since the fresh H-ZSM-5 catalyst did not show any EPR signal, the signals observed on the used catalysts were attributed to organic radicals formed during the MTH/ETH conversion. The concentration of radicals evolved with TOS (Fig. 6); it increased as expected firstly proportionally to the coke content until reaching a steady state, and then decreased concomitantly with the catalyst deactivation (Fig. 1).

## 4 Discussion

At 623 K and under 3.0 MPa of total pressure, H-ZSM-5(40) zeolite converts during a longtime run ( $>100$  h); (Fig. 1) both MeOH and EtOH into hydrocarbons (P,O,N,A – Fig. 3). The evolution of product yields versus TOS depends on the reactant (Fig. 2) and could be related to the nature of coke. Indeed, the nature

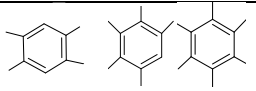
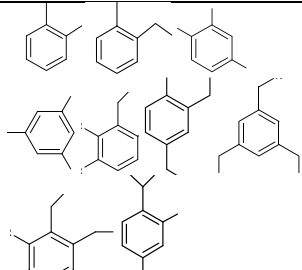
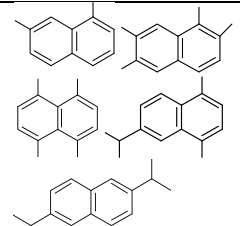
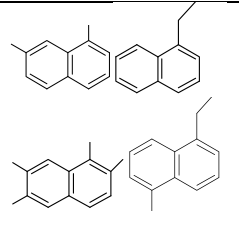
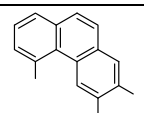
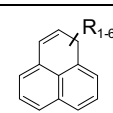
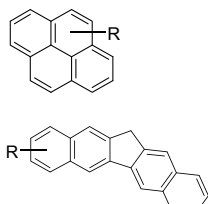
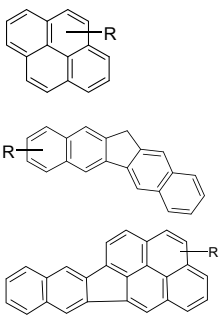


**Fig. 5.** (a) Coke content (wt.%) as a function of time-on-stream (h); (b) residual microporous volumes to nitrogen and (c) residual Brønsted acidity as a function of coke content (wt.%). Tests performed at 623 K on H-ZSM-5 with MeOH ( $\Delta$ ) and EtOH ( $\blacktriangle$ ). ETH data from [20].

of the soluble coke formed on H-ZSM-5 during MTH reaction is composed of polymethyl-benzene (Table 3), whereas with EtOH, it was composed of naphthalenes and phenalenes substituted by methyl and mainly by ethyl groups. The difference between the hydrocarbons molecules trapped inside the zeolite appears after a long run (24 h), while after 2 h reaction Johanson et al. observed no difference on coke composition except ethyl rather to methyl group when ethanol was used instead of methanol [11]. The toxicity of coke molecules ( $\text{Tox}$ ) can be calculated from the above [22–26]: it is the slope of the concentration of protonic sites non accessible to pyridine ( $1 - [\text{PyH}^+]/[\text{PyH}^+]_0$ ) plotted as a function of number of coke molecules per active sites of fresh zeolite ( $C_k/[\text{PyH}^+]_0$ ). Whatever the reactant,  $\text{Tox}$  is slightly lower than 1 (Fig. S.I. 4), meaning that only one coke molecule (alkylphenantrene or alkylpyrene)



**Table 3.** Soluble coke composition after 24 h on stream for MeOH and EtOH. Coke molecules were identified by GC-MS and MALDI-TOF MS techniques.

Family	MeOH 5.8 wt. %	EtOH 6.1 wt. %
<b>A</b>	 ~ 60 %	 ~ 9 %
<b>B</b>	 ~ 30 %	 ~ 30 %
<b>C</b>	 ~ 5 %	 ~ 48 %
<b>D+*</b> (MALDI-TOF)	 ~ 5 %	 ~ 13 %

xx wt. % : Coke content and xx% : % mol determined by GC.

**Table 4.** EPR-CW experimental parameters of the coked H-ZSM-5(40) zeolite with MeOH and EtOH.

Reactant	Coke content(wt.%)	$\Delta H^a$ (G)	g ( $\pm 0.0001$ )	[Rad.] <sup>b</sup> ( $\mu\text{molg}^{-1}$ )
MeOH	5.6	9.3	2.0027	4.4
EtOH	6.1	9.4	2.0026	4.6

<sup>a</sup>EPR linewidth.

<sup>b</sup>Radical concentration per gram of catalyst.

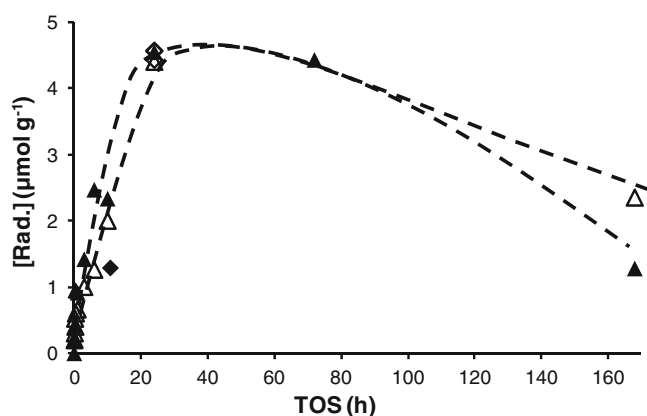


**Fig. 6.** Concentration of radicals ( $\mu\text{mol g}^{-1}$ ) vs. Time-On-Stream (h). Tests performed at 623 K on H-ZSM-5 with MeOH ( $\Delta$ ) and EtOH ( $\blacktriangle$ ). ETH data from [20].

affects one protonic site. The ratio between  $V_R$  (volume really occupied by coke assuming a density equal to  $1.1\text{ g cm}^{-3}$ ) and  $V_A$  (volume apparently occupied by coke deduced from sorption measurements [27]) are always lower than 1 [9,27]. A toxicity slightly lower than 1 and an apparent pore blockage ( $V_R/V_A < 1$ ), can be easily explained [27] by assuming that coke molecules trapped at pore intersections completely block the access to the channels, without necessarily occupying the whole microporous volume. It should be underscored that in spite of the total poisoning of Brønsted acid sites and total pore blocking, the catalyst continued after 100 h (Figs. 1, 5b and 5c) to convert ethanol into  $C_{3+}$  hydrocarbons; EtOH transformation occurs probably by *pore mouth catalysis* [28,29]. Ferreira Madeira et al. [30] showed that passivating the HZSM-5 zeolite ( $\text{Si}/\text{Al} = 16$ ) with TEOS (Tetra Ethyl Ortho Silicate) the reaction clearly does not occur at the outer surface but the reactions are almost certainly done at the pore entry of the channels of the catalyst in “pore mouth”. A study with different zeolites (HY, HBEA, SAPO-34, HZSM-5) with different pore structure should bring on some points of the mechanism. The deactivation is not correlated with the residual concentration of Brønsted acid sites (Fig. 5c), it could be related to the radical concentration (Fig. 6) [31]. The induction period coincides with the appearance of radical by spontaneous ionisation of coke, but the concentration of radicals in Fig. 6 starts to decrease before the deactivation (Fig. 2). The radical disappearance is due to condensation of coke molecules, but the remaining radical concentration seems enough to maintain alcohol conversion into hydrocarbons during several ten hours. The addition to the feed of a radical inhibitor, hydroquinone, accelerated the catalyst deactivation (Fig. 7). MTH was less sensitive to hydroquinone since 2 wt.% were needed to obtain an immediate deactivation while only 1 wt.% was sufficient in the case of EtOH reactant. The deactivation could be related to the consumption of radicals by hydroquinone and not to the modification in the nature and in the location of coke molecules [20]. To prove the importance of radical coke molecules in alcohols transformation, ETH reaction was performed on a low acidic zeolite H-ZSM-5(140) ( $n_{\text{H}^+} = 91\ \mu\text{mol g}^{-1}$ ) doped with a 1-methyl-naphthalene (1MN) in a proportion of one molecule of 1MN *per* Brønsted acid sites (Table 5). 1MN could be considered as a radical precursor [26,33]. The presence of 1MN enhanced both the yield of  $C_{3+}$  (85 versus 99% after 2 hours) and the catalyst stability (53 against 79% after 24 hours) probably due to higher concentration of radicals ( $0.93$  versus  $1.8\ \mu\text{mol.g}^{-1}$ , Table 5).

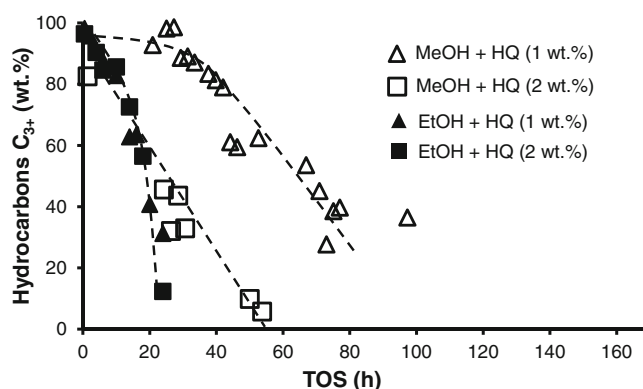


**Fig. 7.** Impact of HQ on the conversion of MeOH (white symbol) and EtOH (black symbol) into hydrocarbons  $C_{3+}$ .

**Table 5.** Impact of 1-methylnaphthalene (1-MN) on the  $C_{3+}$  yield and on the radical content of H-ZSM-5(140).

	Coke content (wt. %)	$C_{H+}$ ( $\mu\text{molg}^{-1}$ )	Yield of $C_3^+$ (%)		[Rad.] ( $\mu\text{molg}^{-1}$ )
TOS (h)	0	0	2	24	24
H-ZSM-5(140)	0	90	85	53	0.93
H-ZSM-5(140) +1-MN	1.1	0	99	79	1.8

Whatever the reactant, the products distribution (Fig. 3) in MTH and ETH is characterized by two maxima at 4 ( $P_4$  or  $O_4$ ) and 8–9 carbon number. Indeed, polyalkylbenzenes, frequently referred to as hydrocarbon pool species, in particular hexamethylbenzene and heptamethylbenzene [34,35] could undergo molecular rearrangement via the “paring reaction” which explain the formation of ( $P_4$  or  $O_4$  and  $A_8$ – $A_9$  carbon number in greater proportion [36–38]. But, it is unlikely that aromatics and olefins come simultaneously from hydrocarbon pool mechanism owing to the high number of steps it demands: a) addition, cyclization and hydrogen transfer (aromatic ring formation); b) aromatic ring alkylation by alcohols (polyalkylbenzenes formation); c) paring reaction; (d) products desorption (acid site freeing). In addition, to respect the product distribution in the case of MTH, aromatics must undergo the steps b and c at least 3 times before that they desorb. Since with MeOH or EtOH (or ethylene), identical compounds are produced (Fig. 3) with same selectivity, it can be assumed that the transformation pathway of these reactants occurs with a Common Reaction Intermediate (CRI) which are probably propene ( $O_3$ ) or butene ( $O_4$ ) [39]. Indeed, the transformation of isopropanol (*i*-PrOH) and butan-1-ol (*n*-BuOH), on H-ZSM-5(40) at 623 K, give the same hydrocarbons than those obtained with MeOH and EtOH and moreover, in the same proportions (Fig. 8). So, it can be concluded that propene and butene are the CRI. The MTH/ETH reactions result of two successive mechanisms (Fig. 9): conversion of the alcohols to the olefins (propene and butene) *via* hydrocarbon pool that occurs at the zeolite channel intersection, follows in pore mouths by inter-conversion of the olefins *via* “conjunct polymerization” as described by H. Pines [40] and J. Vadrine [41]. This dual cycle concept was already proposed by Olsbye et al. in 2006 [42] and further refined in 2007 [43], to explain the concomitance of the formation of aromatics with light olefins during MTH over H-ZSM-5 zeolite. The first cycle is based on arene methylation /dealkylation as contributors to alkene

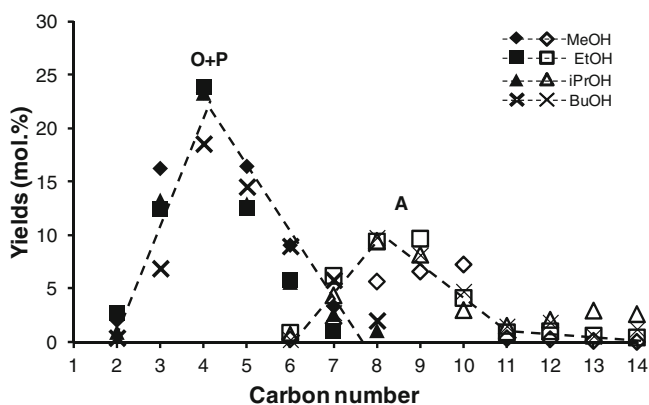


**Fig. 8.** Product distribution: Olefins + Paraffins (O+P)<sub>n</sub> (complete symbol) and Aromatics (A<sub>n</sub>) (empty symbol) as a function of carbon number. Tests performed at 623 K on H-ZSM-5 with MeOH (◆,◇), EtOH (■,□), iPrOH (▲,△) and BuOH (× ×).

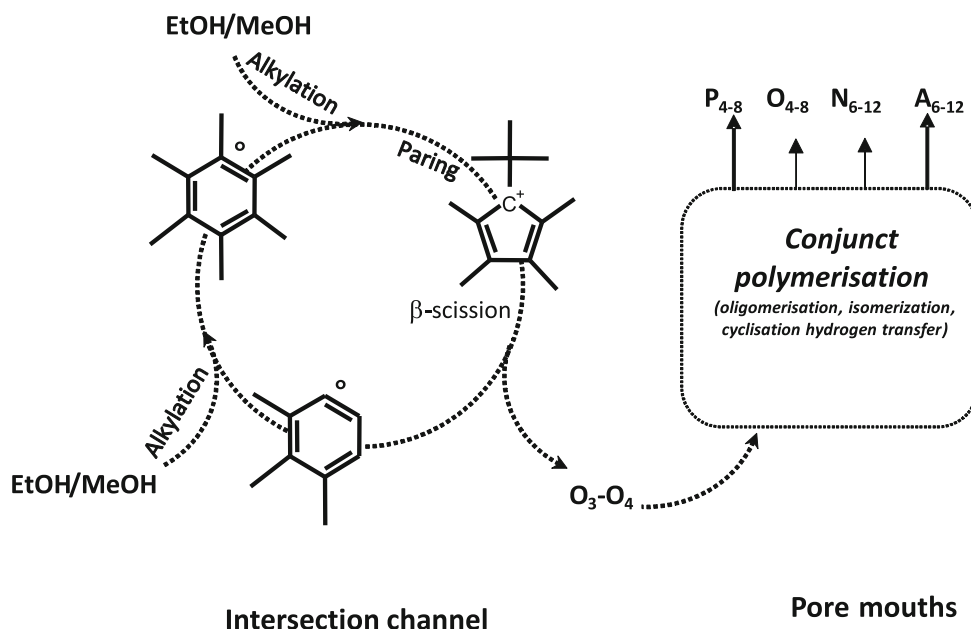


**Fig. 9.** Suggested dual cycle concept for the conversion of methanol and ethanol over H-ZSM-5 zeolite into Aromatics (A) and light Olefins (O).

formation and the second on alkene methylation/cracking undergoing to formation of aromatics. The authors attributed the deactivation to coke formation on the external surface whereas in our case; the cause of the deactivation was assumed to be related to change in the coke composition which was characterized by the decrease of concentration of radical cations; probably by condensation of active coke molecule

(c1ccc2ccccc2c1)<sup>+o</sup> into inert molecule with the reactant (R-c1ccc2ccccc2c1). In MTH/ETH, the role of coke is paradoxical, it acts both as a poison of acid sites or as an active site of the isomerization reaction. The radicals could be considered as a marker of the presence of active hydrocarbon pool.

## 5 Conclusion

A high stability of H-ZSM-5 in the conversion of EtOH and MeOH into hydrocarbons despite its high coke content has been observed at 623 K and under 3.0 MPa. Moreover, same selectivity and products were obtained with both alcohols. However, the unique difference observed is the coke nature formed on zeolite which is related to the more rapid deactivation of EtOH transformation in comparison to MeOH. In fact, during ETH transformation, the coke composition is heavier with naphthalene and phenalene compounds while with MTH, tetra, penta and hexamethylbenzene are mainly formed. In the case of ethanol, the coke molecules could condensate easier into bulkier molecules leading to inactive species and consequently undergoing to faster catalyst deactivation than with methanol. In spite of the total poisoning of Brønsted acid sites and total pore blocking, the catalyst continued after 100 h to convert reactants into C<sub>3+</sub> hydrocarbons. It is assumed that the alcohols transformation occurs probably by *pore mouth catalysis*. Ethanol and methanol are converted into propene and butene *via* hydrocarbon pool. Conjoint polymerization of light alkenes involves the formation of alkanes and aromatics in pore mouths.

Ludovic Pinard thanks the region Poitou-Charentes for its financial support.

## Appendix A. Supplementary data

Supplementary data associated with this article can be found, in the online version at (To be completed).

## References

1. M. Tsuji, T. Goshima, A. Matsushika, S. Kudoh, T. Hoshino, *Cryobiology* **67**, 241 (2013)
2. D. Yuan, K. Rao, P. Relue, S. Varanasi, *Bio. Tech*, **102**, 3246 (2011)
3. C.J. Yoo, D.W. Lee, M.S. Kim, D.J. Moon, K.Y. Lee, *J. Mol. Catal. A: Chem.* **378**, 255 (2013)
4. F.J. Gutiérrez Ortiz, A. Serrera, S. Galera, P. Ollero, *Fuel* **105**, 739 (2013)
5. C.D. Chang, A.J. Silvestri, *J. Catal.* **47**, 249 (1977)
6. K. Ben Tayeb, L. Pinard, N. Touati, H. Vezin, S. Maury, O. Delpoux, *Catal. Comm.* **27**, 119 (2012)
7. M. Bjørgen, U. Olsbye, D. Petersen, S. Kolboe, *J. Catal.* **221**, 1 (2004)
8. I. Dahl, S. Kolboe, *Catal. Lett.* **20**, 329 (1993)
9. F.F. Madeira, K. Ben Tayeb, L. Pinard, H. Vezin, S. Maury, N. Cadran, *Appl. Catal. A: Gen.* **443-444**, 171 (2012)
10. F.F. Madeira, N.S. Gnep, P. Magnoux, S. Maury, N. Cadran, *Appl. Catal. A: Gen.* **367**, 39 (2009)
11. R. Johansson, S. Hruby, J. Rass-Hansen, C. Christensen, *Catal. Lett.* **127**, 1 (2009)
12. L. Matachowski, M. Zimowska, D. Mucha, T. Machej, *Appl. Catal. B: Env.* **123-124**, 448 (2012)
13. K. Ramasamy, Y. Wang, *J. Ener. Chem.* **22**, 65 (2013)
14. V.S. Nayak, V.R. Choudhary, *Appl. Catal.* **9**, 251 (1984)
15. U. Olsbye, S. Svelle, M. Bjørgen, P. Beato, T.V.W. Janssens, F. Joensen, S. Bordiga, K. P. Lillerud, *Angew. Chem. Int. Ed.* **51**, 5810 (2012)
16. K. Hemelsoet, J. Van der Mynsbrugge, K. De Wispelaere, M. Waroquier, V. Van Speybroeck, *Chem. Phys. Chem.* **14**, 1526 (2013)
17. I.M. Dahl, S. Kolboe, *J. Catal.* **149**, 458 (1994)
18. I.M. Dahl, S. Kolboe, *J. Catal.* **161**, 304 (1996)

19. S.J. Kim, H.G. Jang, J.K. Lee, H.K. Min, S.B. Hong, G. Seo, *Chem. Comm.* **47**, 9498 (2011)
20. L. Pinard, K. Ben Tayeb, S. Hamieh, H. Vezin, C. Canaff, S. Maury, O. Delpoux, Y. Pouilloux, *Catal. Today* **218-219**, 57 (2013)
21. L. Pinard, S. Hamieh, C. Canaff, F. Ferreira Madeira, I. Batonneau-Gener, S. Maury, O. Delpoux, K. Ben Tayeb, Y. Pouilloux, H. Vezin, *J. Catal.* **299**, 284 (2013)
22. M. Guisnet, F. Ramôa Ribeiro (eds.), *Deactivation and Regeneration of Zeolite Catalysts* (Imperial College Press, London, 2011)
23. A. Moissette, F. Luchez, C. Brémard, H. Vézin, M. Hureau, *J. Phys. Chem.* **11**, 4286 (2009)
24. H.G. Karge, J.P. Lange, A. Gutsze, M. Laniecki, *J. Catal.* **114**, 144 (1988)
25. S. Marquis, A. Moissette, H. Vezin, C. Bernard, *C.R. Chimie* **8**, 419 (2005)
26. F. Goye, L. Lakiss, Z. Qin, S. Laforge, C. Canaff, M. Tarighi, V. Valtchev, K. Thomas, A. Vicente, J. P. Gilson, Y. Pouilloux, C. Fernandez, L. Pinard, *J. Catal.* **320**, 118 (2014)
27. M. Guisnet, L. Costa, F. Ramôa Ribeiro, *J. Mol. Catal. A: Chem* **305**, 69 (2009)
28. M. Guisnet, *J. Mol. Catal. A: Chem.* **182-183**, 367 (2002)
29. P.G. Menon, *J. Mol. Catal.* **59**, 207 (1990)
30. F. Ferreira Madeira, N.S. Gnep, P. Magnoux, H. Vezin, S. Maury, N. Cadran, *Chem. Eng J.* **161**, 403 (2010)
31. F. Ferreira Madeira, H. Vezin, N.S. Gnep, P. Magnoux, S. Maury, N. Cadran, *ACS Catal.* **1**, 417 (2011)
32. F. Ferreira Madeira, Ph.D. thesis, University of Poitiers, 2009
33. F. Bleken, W. Skistad, K. Barbera, M. Kustova, S. Bordiga, P. Beato, K.P. Lillerud, S. Svelle, U. Olsbye, *Phys. Chem. Chem. Phys.* **13**, 2539 (2011)
34. M. Bjørgen, S. Akyalcin, U. Olsbye, S. Benard, S. Kolboe, S. Svelle, *J. Catal.* **275**, 170 (2010)
35. M. Bjørgen, U. Olsbye, S. Svelle, S. Kolboe, *Catal. Lett.* **93**, 37 (2004)
36. W. von E. Doering, M. Saunders, H.G. Boyton, H.W. Earhart, E.F. Wadley, W.R. Edwards, G. Laber, *Tetrahedron* **4**, 178 (1958)
37. S. Svelle, M. Bjørgen, S. Kolboe, M. Letzel, U. Olsbye, O. Sekiguchi, E. Uggerud, *Catal. Lett.* **109**, 25 (2006)
38. S. Kolboe, S. Svelle, B. Arstad, *J. Phys. Chem. A* **113**, 917 (2009)
39. M. Stöcker, *Micro. Meso. Mat.* **29**, 49 (1999)
40. H. Pines, *The chemistry of Catalytic Hydrocarbon Conversion* (Academic Press, New York, 1981)
41. J.C. Vedrine, P. Dejaifive, E.D. Garbowski, E.G. Derouane, in *Catalysis by Zeolites*, edited by Imelik B. et al., *Stud. Surf. Sci. Catal.* **5**, 29 (Elsevier, 1980)
42. S. Svelle, F. Joensen, J. Nerlov, U. Olsbye, K. -P. Lillerud, S. Kolboe, M. Bjørgen, *J. Am. Chem. Soc.* **128**, 14770 (2006)
43. M. Bjørgen, S. Svelle, F. Joensen, J. Nerlov, S. Kolboe, F. Bonino, L. Palumbo, S. Bordiga, U. Olsbye, *J. Catal.* **249**, 195 (2007)